

## Wetting transitions at soft, sliding interfaces

A. Martin, J. Clain, A. Buguin, and F. Brochard-Wyart

*Institut Curie, Section de Physique et Chimie, Laboratoire de Physico-Chimie des Surfaces et Interface, 11 rue Pierre et Marie Curie, 75231 Paris Cedex 05, France*

(Received 19 June 2001; published 19 February 2002)

We observe (by optical interferometry) the contact of a rubber cap squeezing a nonwetting liquid against a plate moving at velocity  $U$ . At low velocities, the contact is dry. It becomes partially wet above a threshold velocity  $V_{c1}$ , with two symmetrical dry patches on the rear part. Above a second velocity  $V_{c2}$ , the contact is totally wet. This regime  $U > V_{c2}$  corresponds to the hydroplaning of a car (decelerating on a wet road). We interpret the transitions at  $V_{c1}$ ,  $V_{c2}$  in terms of a competition between (a) liquid invasion induced by shear (b) spontaneous dewetting of the liquid (between nonwetable surfaces).

DOI: 10.1103/PhysRevE.65.031605

PACS number(s): 68.15.+e, 68.08.Bc, 81.40.Pq

## INTRODUCTION

The stability of intercalated liquid film at soft interfaces is of crucial interest for many practical applications. In some cases, such as lubricants or the lacrymal film, the rupture of the film may cause damage. On the contrary, when driving on a wet road, the water film has to be fast removed, if one wants to keep the car under control.

Liquid films intercalated between a rubber  $R$  and a solid plane substrate can be prepared by pressing a rubber capsule against a plate through a liquid drop. This technique introduced by Johnson, Kendal, and Roberts (JKR) has been used to observe by interferometry the evolution of the contact versus time [1–3]. The stability of the trapped film depends upon the sign of the spreading coefficient  $S = \gamma_{SR} - (\gamma_{SL} + \gamma_{LR})$ . This coefficient compares interfacial energies between dry ( $\gamma_{SR}$ ) and lubricated ( $\gamma_{SL} + \gamma_{LR}$ ) contacts. If  $S > 0$ , the liquid is a lubricant: the contact at equilibrium remains wet by a thin nanoscopic film and the friction coefficient is very small. On the other hand, if  $S < 0$ , the film is unstable and dewets to achieve a dry contact between the rubber and the solid. Liquids with  $S < 0$  are “triboactive,” i.e., they generate a large liquid-rubber friction. To escape, the liquid must deform the rubber. A characteristic “elastic length,”  $h_0 = |S|/E$  ( $= 10$  nm) describes the competition between surface energy and rubber elasticity. At length larger than  $h_0$ , the elastic energy associated to the rubber deformation plays a major role.

We studied previously the dewetting of metastable liquid films, using the JKR setup in Ref. [3]. The rubber bead, prepared by reticulation of a polymer droplet, was smooth down to at atomic scale. The liquid was water (or fluorinated oil) deposited on a silanated glass. The (negative) spreading coefficient, which is the driving force for dewetting, was measured by monitoring the shape of a droplet trapped at the liquid-rubber interface [4]. The drops, instead of being spherical when exposed to air, have a very flat “penny” shape, when they are embedded in a rubber [5].

When the rubber bead is pressed against the glass plate, the lens is deformed and a flat film of radius  $a$  ( $= 100$   $\mu\text{m}$ ) is formed. At this stage the applied external force  $F$  is maintained constant and is responsible for the drainage of the intercalated film. The evolution of the film thickness  $e$  with

the time  $t$  is well described by a classical Reynolds law [3]. If  $V_R$  is the drainage velocity and  $\eta$  the liquid viscosity, the transfer of mechanical energy into viscous dissipation leads to (omitting numerical coefficients)  $F\dot{e} \approx \eta(V_R/e)^2 ea^2$ . With the volume conservation  $\dot{e}/e \approx V_R/a$ , it leads to  $e \approx [(\eta a^3 V_R)/F]^{1/2}$ , which gives the Reynolds law  $e(t) \approx t^{-1/2}$ . Experimentally,  $e(t) \approx V_R^\alpha$  with  $\alpha = 0.6 \pm 0.05$  slightly larger than 0.5. The deviation is attributed to dimple formation at the rubber surface.

When the thickness  $e$  is in the range of few thousand angströms, dewetting takes place by nucleation and growth of a dry patch. Only very thin films can dewet, because the size of the contact required to induce the dewetting has to be larger than  $R_c \approx e^2/h_0$  ( $\approx 1$   $\mu\text{m}$  for  $e \approx 0.1$   $\mu\text{m}$ ). This applies also to a car driving on a wet road. We have been able to nucleate one single contact and to observe the growth of a dry patch of radius  $R$ , surrounded by a rim that collects liquid. We have interpreted [6] the growth laws by a simple model, based on three assumptions:

(i) The shape of the rim, squeezed at the liquid-rubber interface, is extremely flat. Assuming that its shape is quasi-static, its length  $l$  is related to its thickness  $h$  by the scaling relation  $l = h^2/h_0$  [4,5].

(ii) All the liquid is collected in the rim, liquid conservation imposes  $lh \approx \text{Re}$ .

(iii) The driving force on the rim  $S$  is balanced by the friction force. If one assumes that all the dissipation takes place in the liquid rim moving at velocity  $V = dR/dt$ , and not in the rubber (assumed to be purely elastic), the transfer of surface energy into viscous losses leads to

$$V = \frac{S h}{\sigma l} = \frac{S h_0}{\eta h}.$$

Dewetting starts at a velocity

$$V_d = k_1 \frac{|S| h_0}{\eta e}, \quad (1)$$

where  $k_1$  is a prefactor discussed in Ref. [1].

Here our aim is to study the inverse process: forced wetting of a contact that is initially dry. When we move the glass plate in its plane at a sufficiently large velocity  $U$ , the shear induces a lubrication of the contact. This unbinding may be

dramatic for cars slowing down on a wet road (“hydroplaning”). A positive application is the controlled deposition of intercalated liquid films.

This “forced wetting” has been studied intensively [7–10] in a different case, namely, liquid films between air and a nonwetable substrate. A typical experiment consists to pull out at velocity  $U$ , a plate (or a fiber) immersed in the liquid bath. A critical velocity  $V_c$  separates two regimes (i)  $U < V_c$ , the plate remains dry, (ii)  $U > V_c$ , the plate is wet. The thickness  $e(U)$  of the deposited film is given by the Landau-Levich law [ $e(U) \sim U^{2/3}$ ] [7], and does not depend upon the wettability of the substrate. The transition at  $U = V_c$  is discontinuous. Experimentally [8],  $V_c \propto V^* \theta_E^1$  ( $V^* = \gamma/\eta$  is a characteristic velocity of the liquid of surface tension  $\gamma$ , viscosity  $\eta$ ) scales such as the dewetting velocity [11], in agreement with theoretical predictions [12].

In this paper we provide the quantitative study of the “forced wetting” at soft interfaces, where air is replaced by rubber. We are faced with two questions. (i) Do we have a sharp wetting transition? (ii) How do the thickness and the shape of the lubricated contact depend on  $U$ ?

## EXPERIMENTS

A rubber cap is pressed against a hydrophobic plate through a separating liquid drop. The elastomer, a crosslinked polydimethylsiloxane, behaves similar to a pure elastic medium (Young modulus  $E = 0.74$  MPa). The preparation of the rubber lenses, and the silanization of microscope glass slides are described in Ref. [3]. The liquid, a fluorinated silicone oil [polyfluoroalkylsiloxane (PFAS)], is immiscible with polydimethylsiloxane. The viscosities  $\eta$  range between 1 to 20 Pa.s. We measure  $S$  from the static shape of intercalated droplets  $S = -7.4$  mN/m [4]. The elastomer cap is attached to a micromanipulator. The glass plate is set in the motorized platine of an inverted microscope, and can move in translation at constant velocity  $U$ , ranging from 10 to 500  $\mu\text{m/s}$ . We follow the normal approach of the lens using reflection contrast interferential microscopy [13]. When the bead is not in contact with the plate, we observe Newton rings. When the lens nearly touches the plate, it is deformed. We do not immediately get a dry contact, but rather a flat liquid film of radius  $a \sim 100$   $\mu\text{m}$ . At this stage, we hold the position of the elastomer. The vertical force required for a contact of size  $a$  is relatively strong, and thus well described by the Hertz law [14]

$$a^3 = \frac{9}{16} \frac{F}{E} R_b, \quad (2)$$

where  $R_b$  is the radius of the lens ( $R_b \sim 1$  mm). The film, squeezed by the rubber, gets thinner and suddenly dewets. The contact area at equilibrium is then dry.

At this stage, we shear the dry contact by displacing the glass plate horizontally at velocity  $U$ , while the elastomer lens is fixed. We observe three steady state regimes, shown in Fig. 1, separated by two critical wetting velocities  $V_{c1}$  and  $V_{c2}$ . (a) At low velocities  $U < V_{c1}$  the rubber remains in contact with the glass. The contact area is somewhat de-

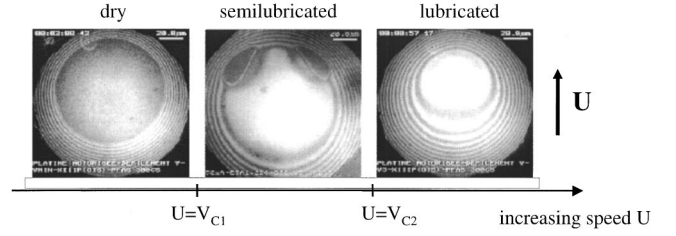


FIG. 1. Regimes of forced wetting observed (by RICM) in the sliding rubber/liquid/glass contact versus increasing sliding speed  $U$  (the arrow indicates the direction of the glass plate velocity).

formed [Fig. 1(a)], but the contact remains “dry.” (b) At intermediate velocities  $V_{c1} < U < V_{c2}$  the contact is restricted to two small dry patches [Fig. 1(c)]. We call this the semilubricated regime. (c) At high velocities  $U > V_{c2}$  the contact is lost [Fig. 1(c)], this is a case of full lubrication.

The velocities  $V_{c1}, V_{c2}$  depend on the viscosity  $\eta$  with the same exponent  $\beta$ ,

$$V_{c1} \propto \eta^{-\beta}, \quad V_{c2} \propto \eta^{-\beta}, \quad (3)$$

with  $\beta = 0.75 \pm 0.02$ . Both  $V_{c1}$  and  $V_{c2}$  are independent of the size (a) of the original contact.

Above  $V_{c2}$ , a film of liquid is forced at the liquid-rubber interface. The profiles of the liquid-rubber interface derived from interferometry are shown in Fig. 2. In our velocity range, the interface is essentially planar, but tilted by a small angle  $\theta = (e_{\text{in}} - e_{\text{out}})/2a$  (ranging from  $10^{-3}$  to  $10^{-2}$  rad), where  $e_{\text{in}}$  and  $e_{\text{out}}$  are the thicknesses of the liquid at both ends [Fig. 2(b)]. The average thickness is  $e(U) = (e_{\text{in}} + e_{\text{out}})/2$ . We find

$$\theta = \text{const} \times \frac{e}{a} \quad (\text{const} = 0.35 \pm 0.1), \quad (4)$$

$$e(U) = \text{const} \times \eta^{\alpha_1} U^{\alpha_2} \quad (\alpha_1 = 0.47 \pm 0.05, \alpha_2 = 0.57 \pm 0.05). \quad (5)$$

Ultimately, at very high velocities, the structure becomes more complex. A zone of constriction appears at the rear end, as already observed by Reynolds [15] (“the horse shoe effect”).

## INTERPRETATION

We now analyze the film thickening under shear and the critical velocities  $V_{c1}$  and  $V_{c2}$ .

Elastohydrodynamic profiles have been analyzed by many authors, mainly in connection with the lubrication of metal/metal contacts (for a review see Ref. [16]). But they do not provide analytical solutions. Here we present a cruder model of lubrication, which accounts for most of the facts described above.

We derive the thickness  $e$  by a balance between Reynolds drainage [16] and forced flows.

(a) Reynolds flow, when a film of thickness  $e$  is squeezed by a force  $F$ , it expels the fluid with an outward velocity  $V_R(e)$ . This was discussed in the Introduction,

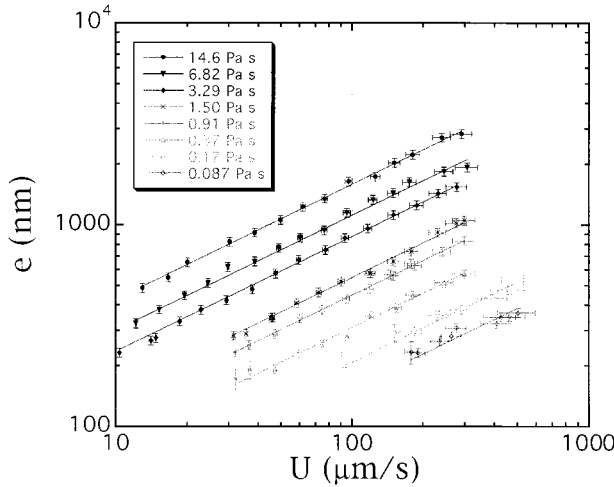
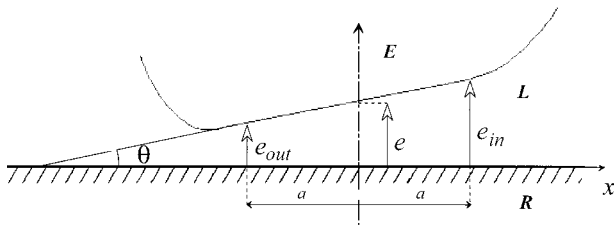
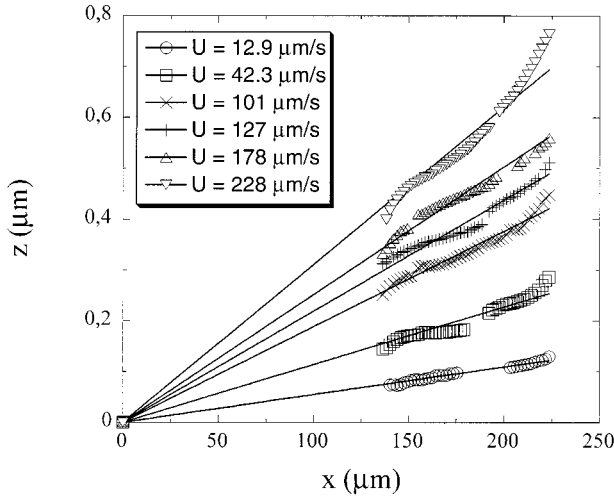


FIG. 2. Characterization of the lubricated regime. (a) Profiles of the rubber measured by interferometry along the  $U$  axis for increasing sliding speed  $U$  in the lubricated regime ( $U > V_{c2}$ ). (b) Schematic picture of the lubricated contact: thin liquid wedge [thickness  $e(U)$ ] between slightly tilted plates [angle  $\theta(U)$ ]. The lateral size  $a$  is imposed by the applied (constant) load. (c) Film thickness  $e(U)$  plotted as a function of sliding speed for a series of PFAS oils.

$$V_R(e) = \frac{Fe^2}{\eta a^3}. \quad (6)$$

(b) Inward flow with a velocity comparable to  $U$ .

In steady state the two effects balance exactly ( $V_R = U$ ) and we expect

$$e(U) \cong \left( \frac{\eta a^3 U}{F} \right)^{1/2} = \left( \frac{\eta U R_b}{E} \right)^{1/2}. \quad (7)$$

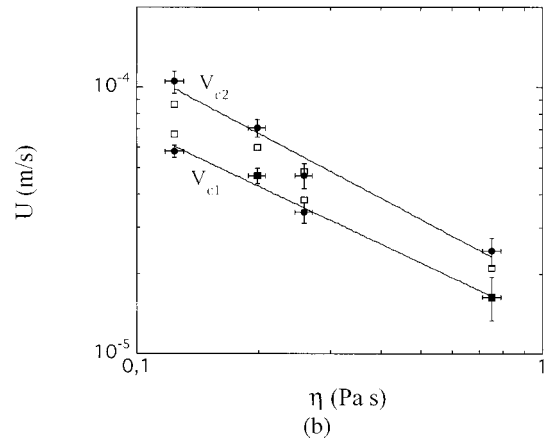
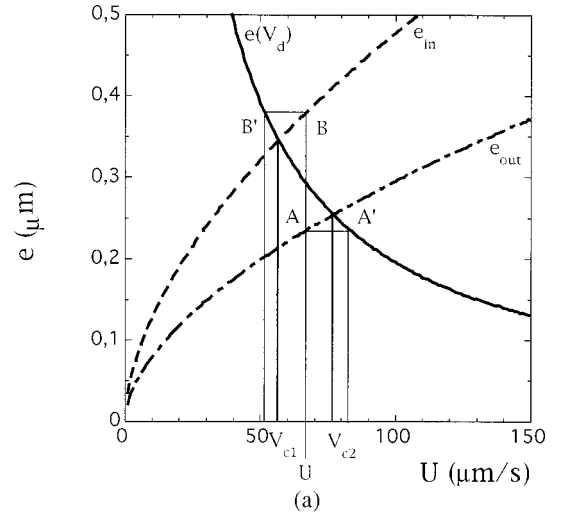


FIG. 3. Critical velocities of the wetting transitions  $V_{c1}$  and  $V_{c2}$ . (a) Construction of the velocities  $V_{c1}$  and  $V_{c2}$ . The plot  $e(v_d)$  gives the thickness of the film that dewets at velocity  $V_d = U$  (deduced from datas of Ref. [1]).  $e_{in}$  and  $e_{out}$  are the thicknesses of the liquid wedge at both ends. For a sliding velocity  $U$ , we deduce  $e_{out}$  (point A) and  $e_{in}$  (point B) and the respective dewetting velocities  $v_d(e_{out})$  (point A') and  $v_d(e_{in})$  (point B'). If  $v_d > U$  (point A'), the contact is dry. If  $v_d < U$  (point B'), the contact is wet. If  $U < V_{c1}$ , the construction shows that  $v_d(e_{in}) > U$ , dewetting dominates at both ends. If  $U > V_{c2}$ , dewetting is weak. If  $V_{c1} < U < V_{c2}$ ,  $v_d(e_{out}) < U$ , dewetting dominates only in the thinner part. (b) Direct measurements of  $V_{c1}$  and  $V_{c2}$  (●) for oils of various viscosities, compared to the values obtained by construction (□).

Experimentally we find  $e(U) \approx U^{0.57}$ . Deviations from our simple exponents ( $\alpha_2 = 0.57$  instead of 0.5) are probably due to small deviations from a planar plate [19].

We can also derive the tilt angle from a balance between hydrodynamic lift and the applied vertical force  $F$ . In our conditions the surface of the elastomer is essentially a slightly tilted plate [Fig. 2(c)] and the hydrodynamic lift force can be written simply as [17,18]

$$F_b = 6 \eta a \frac{U}{\theta^2} \left[ \ln \left( \frac{2 + \Delta}{2 - \Delta} \right) - \Delta \right], \quad (8)$$

where  $\Delta = (e_{in} - e_{out})/e$ .

This force  $F_h$  must be equal to the applied force [Eq. (2)]  $F_h = F$ . Using Eq. (7) this leads to

$$\theta = \text{const} \frac{e}{a}, \quad (9)$$

or equivalently to  $\Delta = \text{const}$ . This scaling law Eq. (9) is well verified by our data [Eq. (4)].

With this simple scaling model of thickening  $e(U)$ , we can derive the critical velocities. Just as Eq. (7) can be understood as a competition between external flow and Reynolds flow, we can understand the critical velocities by a competition between forced wetting and dewetting.

We know from earlier experiments on dewetting between glass and rubber without shear [1] that the dewetting velocity for a gap of thickness  $e$  is

$$V_d(e) = \frac{k_1}{\eta} \frac{|S|^2}{Ee}, \quad (10)$$

where  $E$  is the elastic modulus of the rubber and  $k_1$  a prefactor discussed in Ref. [1].

We plot in Fig. 3(a) the experimental curves for  $e_{\text{in}}(U)$  and  $e_{\text{out}}(U)$  and also the curve  $e(V_d = U)$  corresponding to Eq. (9). The speed  $V_{c1}$  corresponds to  $e_{\text{in}}(U) = e(V_d = U)$ . The speed  $V_{c2}$  corresponds to  $e_{\text{out}}(U) = e(V_d = U)$ .

If  $U < V_{c1}$  the dewetting velocity is larger than  $U$  at all thicknesses in the interval  $(e_{\text{in}}(U), e_{\text{out}}(U))$  and the contact remains dry. If  $U > V_{c2}$  dewetting is slower than  $U$  at both ends then the flow penetrates. If  $V_{c1} < U < V_{c2}$  dewetting dominates at the rear end [ $V_d(e_{\text{out}}) > U$ ] but dewetting is weak at the entry [ $V_d(e_{\text{in}}) < U$ ], then the contact is semilubricated.

We have compared the measurements of  $V_{c1}$  and  $V_{c2}$  to this construction for oils of various viscosities, the agreement is good [Fig. 3(b)].

Our simple description leads to a scaling prediction for the critical velocities,

$$V_{c1} \propto V_{c2} \propto \frac{|S|}{\eta} \left( \frac{|S|}{ER_b} \right)^{1/3}. \quad (11)$$

Experimentally we do find that  $V_{c1}$  and  $V_{c2}$  are independent of the size ( $a$ ) of the initial contact. On the other hand, the dependence upon viscosity ( $\beta = 0.75 \pm 0.2$ ) is in mediocre agreement with the predicted value ( $\beta = 1$ ).

Thus we understand relatively simply the forced wetting of triboactive liquid at soft interfaces. Our model becomes very rough at high velocities when horse shoe shapes occur, then the existing numerical calculations on elastohydrodynamic profiles with wetting fluids are necessary. But our approach does give a physical guideline at moderate velocities.

We have not been able to measure the same transitions for pure water, because the corresponding velocities are very large ( $\sim 1$  m/s from our model). But the principles should remain valid, and useful for discussions on (a) hydroplaning of cars (b) forced wetting by soft instruments, as it is found in many painting applications.

#### ACKNOWLEDGMENT

The authors are grateful to P.G. de Gennes for helpful discussions.

- 
- [1] A. D. Roberts, *Tribol. Int.* **10**, 115 (1977).  
 [2] A. D. Roberts, *J. Phys. D* **4**, 423 (1971).  
 [3] P. Martin and F. Brochard-Wyart, *Phys. Rev. Lett.* **80**, 3296 (1998).  
 [4] P. Martin, P. Silberzan, and F. Brochard-Wyart, *Langmuir* **13**, 4910 (1997).  
 [5] J. N. Sneddon, *Proc. R. Soc. London, Ser. A* **187**, 229 (1946).  
 [6] F. Brochard-Wyart and P. G. de Gennes, *J. Phys.: Condens. Matter* **6**, A9 (1994).  
 [7] L. Landau and B. Levich, *Acta Physicochim. URSS* **17**, 42 (1942).  
 [8] R. V. Sedev and J. G. Petrov, *Colloids Surf.* **17**, 283 (1986); D. Quéré, *C. R. Acad. Sci. Paris* **313**, 313 (1991).  
 [9] T. Podgorski, J. M. Fleyselles, and L. Limat, *Phys. Rev. Lett.* **87**, 036102 (2001).  
 [10] H. A. Stone, L. Limat, F. K. Wilsonand, and T. Podgorski, *C. R. Acad. Sci. Paris* (to be published).  
 [11] C. Redon, F. Brochard-Wyart, and F. Rondelez, *Phys. Rev. Lett.* **66**, 715 (1991); O. Reynolds, *Philos. Trans. R. Soc. London* **117**, 157 (1886).  
 [12] J. F. Joanny and P. G. de Gennes, *C.R. Acad. Sci. Ser. II: Mec., Phys., Chim., Sci Terra Unvers* **299**, 279 (1984); P. G. de Gennes, *Rev. Mod. Phys.* **57**, 827 (1985).  
 [13] J. Rädler and E. Sackmann, *J. Phys. II* **3**, 727 (1993).  
 [14] H. Hertz, *Miscellaneous Papers* (McMillan, London, 1896); K. L. Johnson, K. Kendall, and A. D. Roberts, *Proc. R. Soc. London, Ser. A* **324**, 301 (1971); M. K. Chaudury and G. Whitesides, *Langmuir* **7**, 1013 (1991).  
 [15] O. Reynolds, *Philos. Trans. R. Soc. London* **177**, 157 (1886).  
 [16] A. D. Roberts and P. Tabor, *Proc. R. Soc. London, Ser. A* **325**, 323 (1971); *Discuss. Faraday Soc.* **1**, 243 (1970).  
 [17] J. M. Georges, *Frottement, Usure et Lubrification* (CNRS, Paris, 1999).  
 [18] E. Guyon and J. P. Hulin, *Physical Hydrodynamic* (EDP Sciences, Paris, 1991), p. 363; G. K. Batchelor, *An Introduction to Fluids Dynamics* (Cambridge Library, Cambridge, 2000).  
 [19] Note: if we take the experimental law observed for the drainage  $e \approx V_R^{0.6}$  [3], we find  $e(U) \approx U^{0.6}$  in good agreement with the thickening law Eq. (5).